Theoretical research on proton halos in exotic nuclei *

Dong-Dong Ni(倪冬冬)[1;1)] Zhong-Zhou Ren(任中洲)[2,3,4;2)]

[1] Space Science Institute, Macau University of Science and Technology, Macao, China
[2] Department of Physics, Institute of Acoustics, Nanjing University, Nanjing 210093, China
[3] School of Physics Science and Engineering, Tongji University, Shanghai 200092, China
[4] Center of Theoretical Nuclear Physics, National Laboratory of Heavy-Ion Accelerator, Lanzhou 730000, China

Abstract: Very neutron-deficient nuclei are investigated with Woods-Saxon potentials, especially the newly measured $A=2Z-1$ nucleus ^{65}As [X.L. Tu et al., Phys. Rev. Lett. **106**, 112501 (2011)], where the experimental proton separation energy is obtained as -90(85) keV for the first time. Careful consideration is given to quasibound protons with outgoing Coulomb wave boundary conditions. The observed proton halos in the first excited state of ^{17}F and in the ground states of ^{26,27,28}P are reproduced well, and predictions of proton halos are made for the ground states of ^{56,57}Cu and ^{65}As. The sensitivity of the results to the proton separation energy is discussed in detail, together with the effect of the $\ell=1$ centrifugal barrier on proton halos.

Keywords: proton halo, valence proton, quasibound state

PACS: 21.10.Ft, 21.10.Gv, 21.10.Pc **DOI:** 10.1088/1674-1137/41/11/114104

1 Introduction

The search for the limits of stability is one of the focal subjects in contemporary nuclear physics. The proton drip line defines one of the fundamental limits of nuclear stability. Nuclei lying beyond this line generally have negative proton separation energies with a natural tendency to emit a proton, or large β-decay energies with a natural tendency to transform protons into neutrons [1, 2]. Nuclei near the line are characterized by one or more loosely bound protons, leading to some phenomena of great interest, such as proton halos and proton skins [3–5]. Furthermore, such exotic structure properties have a great influence on nuclear decay properties [6, 7].

In very proton-rich nuclei, the external wave function of the weakly bound protons generally has a large amplitude, so that it has non-negligible contributions to nuclear structure properties. This is in great contrast to nuclei near the β-stable line, where the amplitude of the external wave function is too small to be considered in the evaluation of various physical quantities. The experimental search for proton halos in very neutron-deficient nuclei is of great interest. From the theoretical viewpoint, various approaches have been made to calculate the properties of proton halos, including relativistic mean-field (RMF) theory [8–11], the shell model (SM) with improved ingredients [12], *ab initio* calculations [13], and so on. Self-consistent RMF calculations are essential to give a unified description of ground-state properties of halo nuclei, such as binding energies and charge radii [8–11, 14–17]. Various RMF models with improved ingredients have been developed for halo structures in exotic nuclei, such as relativistic continuum Hartree Bogoliubov (RCHB) models [14, 15] and deformed relativistic Hartree Bogoliubov (DRHB) models [16, 17]. Pairing correlations and continuum effects were considered in their calculations [14–17]. Neutron halos have been widely investigated within these models, but studies on proton halos are rare owing to the existence of the Coulomb barrier [11].

Experimentally, direct mass measurements of the $A=2Z-1$ nuclei ^{63}Ge, ^{65}As, ^{67}Se, and ^{71}Kr were made in 2011 [18]. One important achievement is that the proton separation energy of ^{65}As was measured as S_p=-90(85) keV, which demonstrates that this nucleus is only slightly proton unbound. Additionally, based on RMF calculations and systematic analysis [19], the spin-parity of $3/2^-$ is tentatively assigned to the ground state of ^{65}As. This suggests that the last valence proton in ^{65}As exhibits low angular momentum $\ell=1$. As we know, the formation of proton-halo structure mainly results from one or more

Received 11 July 2017

∗ Supported by Science and Technology Development Fund of Macau (007/2016/A1, 039/2013/A2), National Natural Science Foundation of China (11535004, 11035001, 11375086, 11105079, 10735010, 10975072, 11175085, 11235001), National Major State Basic Research and Development of China (2016YFE0129300) and Research Fund of Doctoral Point (RFDP) (20100091110028)

1) E-mail: dongdongnick@gmail.com

2) E-mail: zren@nju.edu.cn

loosely bound protons with small proton separation energies S_p and low angular momentum ℓ. The nucleus ^{65}As could be a perfect research object for the proton-halo structure. As far as we know, there has been no study on proton-rich nuclei with quasibound protons. It is therefore very interesting to provide a straightforward theoretical study of ^{65}As, which may be useful for further insights into the nature of the halo structure. In this work, we will first review proton halos in the first excited state of ^{17}F and in the ground states of ^{26,27,28}P. We will then predict whether or not there are proton halos in ^{65}As.

2 Theoretical framework

The picture we consider here is essentially based on mean field theory. The mean field potential is approximated as the sum of the average Woods-Saxon potential and the spin-orbit term:

$$V=V_N f(r)+V_{\rm so}(2\ell\cdot\mathbf{s})\frac{1}{r}\frac{\rm d}{{\rm d}r}f(r), \tag{1}$$

where $f(r)=\left\{1+\exp[(r-R)/a]\right\}^{-1}$ with $R=r_0A^{1/3}$, and A is the mass number of the nucleus under investigation. The Chepurnov Woods-Saxon parameter set presented in Ref. [20] is adopted here: $r_0=1.24$ fm and $a=0.63$ fm. It was mainly fitted to the experimental data available at the time on spherical nuclei, including lighter ones. Also, the depth of the central potential is parameterized as [20]

$$V_N=V_0[1\pm0.63(N-Z)/(N+Z)], \tag{2}$$

where N and Z are, respectively, the neutron number and atomic number of the nucleus under investigation, the plus sign is for protons and the minus sign for neutrons. The depth V_0 has not been taken from Ref. [20] but rather adjusted to reproduce the experimental proton separation energy, as discussed below. For the strength of the spin-orbit potential, following Ref. [2], the simple ansatz $V_{\rm so}=-0.20V_N$ is used. For the case of protons, the Coulomb potential is taken in the usual form of a homogeneously charged sphere [with the nuclear charge $(Z-1)e$ and the radius $R_{\rm C}$] as

$$\begin{aligned} V_{\rm C}(r)&=\frac{(Z-1)e^2}{r}, && r>R_{\rm C},\\ V_{\rm C}(r)&=\frac{(Z-1)e^2}{2R_{\rm C}}\left[3-\left(r/R_{\rm C}\right)^2\right], && r\leqslant R_{\rm C}, \end{aligned} \tag{3}$$

with $R_{\rm C}=1.22(A-1)^{1/3}$ (fm). Considering the difficulty and complication in dealing with the nuclear many-body problem, no correlations between nucleons are taken into account for simplicity.

The main focus of our calculation is on the last valence proton, which is usually weakly bound or even slightly unbound. First, the single-particle energy of the last valence proton is determined from the proton separation energy $S_{\rm p}$, that is, $\varepsilon_{\ell j}=B(A-1,Z-1)-B(A,Z)=-S_{\rm p}(A,Z)$. The corresponding wave function is then obtained by numerically integrating the radial Schrödinger equation,

$$\left[-\frac{\hbar^2}{2\mu}\frac{{\rm d}^2}{{\rm d}r^2}+V+\frac{\ell(\ell+1)\hbar^2}{2\mu r^2}\right]u_{n\ell j}(r)=\varepsilon_{\ell j}u_{n\ell j}(r). \tag{4}$$

At this point, the potential depth V_0 is adjusted to reproduce the experimental value $\varepsilon_{\ell j}=-S_{\rm p}$, and the radial single-particle wave function of the bound or quasibound state is numerically computed by matching it to the Whittaker or Coulomb wave function in the following form

$$\begin{cases} u_{n\ell j}(R)=N_{\ell j}\ W_{-\eta,\ell+1/2}(2kR) & \text{for bound states,}\\ u_{n\ell j}(R)=N_{\ell j}\ G_\ell(kR) & \text{for quasibound states,} \end{cases} \tag{5}$$

where $N_{\ell j}$ are normalization constants, the wave number k is determined by the expression $k=\sqrt{2\mu|\varepsilon_{\ell j}|}/\hbar$, and the Sommerfeld parameter η is given by $\eta=\mu(Z-1)e^2/(\hbar k)$. The radial Eq. (4) is solved by the shooting method in the radial space of 0−100 fm where the mesh size is taken as 0.05 fm. Next, with the fixed potential depth V_0, the single-particle energies and wave functions of the lower-lying single-particle orbits are achieved by solving Eq. (4) in a similar manner.

3 Results and discussion

First, let us consider the first excited state of ^{17}F, which is well known for its halo structure [21]. The $5/2^+$ state in ^{17}F is weakly bound by roughly 600 keV. The calculated single-particle energy for this state agrees well with the experimental value, as shown in Table 1. Furthermore, the root-mean-square (rms) radii of the protons in the $1s_{1/2}$ and $1d_{5/2}$ states are evaluated at 5.381 and 3.732 fm, respectively. These values are very close to the values of 5.333 and 3.698 fm in Ref. [21]. In Table 1, direct comparison of the rms radii shows that the $R(2s_{1/2})$ value is apparently larger than the $R_{\rm p}$ and $R(1d_{5/2})$ values. This clearly indicates that there is a proton halo in the excited state of ^{17}F.

Then, we investigate the proton-halo structure of the $Z=15$ neutron-deficient isotopes ^{26,27,28}P. It is known from available experimental cases that there is no proton halo in the ground state of ^{25}Al, while the ground states of ^{26,27,28}P are characterized by the proton-halo structure [22–24]. For comparison, the numerical results of ^{25}Al and ^{26,27,28}P are listed in Table 1. One can see that the last valence protons in ^{25}Al and in ^{26,27,28}P occupy the $1d_{5/2}$ and $2s_{1/2}$ orbits, respectively. The $R(1d_{5/2})$ value is not much larger than the $R_{\rm p}$ value in ^{25}Al, while the $R(2s_{1/2})$ values are quite a lot larger than the $R_{\rm p}$ values

in ^{26,27,28}P. The underlying reason for this is that the valence $1d_{5/2}$ orbit in ^{25}Al has a higher centrifugal barrier $\ell=2$ as well as a larger binding energy -2.2716(5) MeV, restricting the formation of proton halos. In addition, in proceeding from ^{26}P to ^{27}P to ^{28}P, the proton separation energy increases greatly but the $R(2s_{1/2})$ value decreases relatively smoothly. This suggests that the halo-proton rms radius is not so sensitive to the proton separation energy. This is quite consistent with the conclusion of Refs. [8, 9, 12]. A detailed discussion about this is presented at the end of this work.

Table 1. Structure properties calculated in the Woods-Saxon potential with fixed proton separation energies for the first excited state of ^{17}F and the ground states of ^{25}Al, ^{26,27,28}P. The energies are in MeV, and the radii are in fm. The values with error bars are the single-particle energies of the last valence proton $\varepsilon_{\ell j}=-S_{\rm p}(A,Z)$ and they are used to determine the potential depth V_0 in the Woods-Saxon potential.

	^{17}F*	^{25}Al	^{26}P	^{27}P	^{28}P
R_m	2.833	3.092	3.154	3.147	3.130
R_n	2.531	2.982	2.826	2.912	2.973
$R_{\rm p}$	3.077	3.190	3.374	3.323	3.259
$R(2s_{1/2})$	5.381	–	4.666	4.382	4.110
$R(1d_{5/2})$	3.732	3.701	3.736	3.682	3.610
$\varepsilon(2s_{1/2})$(p)	-0.10494(25)	–	-0.140(200)[1]	-0.870(26)	-2.0522(12)
$\varepsilon(1d_{5/2})$(p)	-0.657	-2.27138(7)	-1.782	-2.778	-4.303
$\varepsilon(1p_{1/2})$(p)	-10.734	-11.582	-10.912	-11.968	-13.622
$\varepsilon(1p_{3/2})$(p)	-13.794	-13.771	-13.026	-14.053	-15.709
$\varepsilon(1s_{1/2})$(p)	-27.348	-25.046	-24.006	-24.972	-26.654
$\varepsilon(1d_{5/2})$(n)	-6.416	-8.866	-14.254	-13.386	-13.305
$\varepsilon(1p_{1/2})$(n)	-17.555	-19.088	-24.994	-23.898	-23.676
$\varepsilon(1p_{3/2})$(n)	-20.868	-21.360	-27.468	-26.218	-25.894
$\varepsilon(1s_{1/2})$(n)	-35.464	-33.495	-40.102	-38.473	-37.886

[1] The values are based on the Ame2012 atomic mass systematics [25].

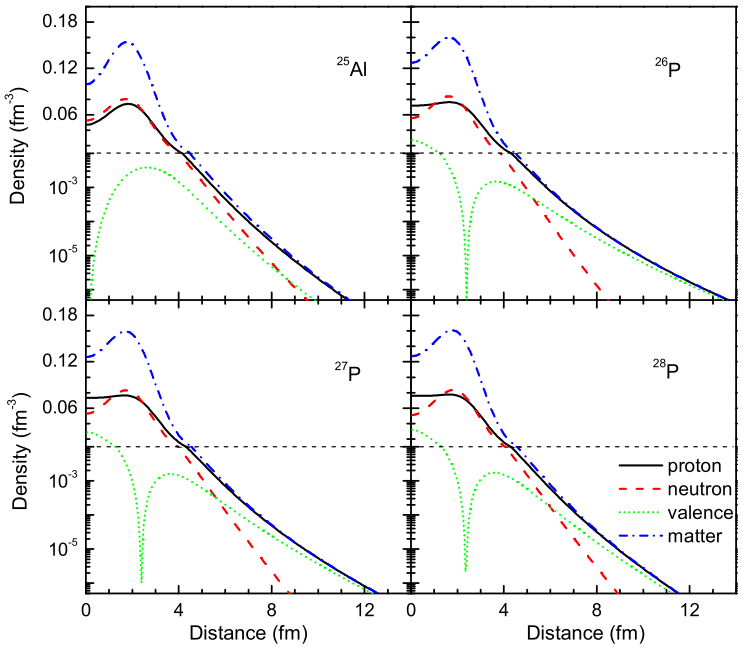

Fig. 1. (color online) Radial density probability distributions of all protons, all neutrons, the last valence proton, and nuclear matter, for the ground states of ^{26,27,28}P, compared with those for the ground state of ^{25}Al. On the vertical axis, the density range of less than 0.01 g/cm^3 is shown in the logarithmic scale while the density range of more than 0.01 g/cm^3 is in the linear scale, and they are distinguished by thin dashed horizontal lines.

For the sake of clarity, Fig. 1 shows the radial density distributions of all protons, all neutrons, the last valence proton, and nuclear matter for the ground states of ^{25}Al and ^{26,27,28}P. There is a long tail in the density distribution of all protons for ^{26,27,28}P, which is mainly contributed by the last valence proton. That is, the proton-halo structure is in evidence. On close inspection, it is also revealed that the proton-halo character becomes subdued from ^{26}P to ^{27}P, followed by ^{28}P. For ^{25}Al, the situation is exactly opposite to those of ^{26,27,28}P, showing that proton halos do not exist in its ground state.

Next, let us turn back to the newly measured nucleus ^{65}As. The experimental measurements show that the $S_{\rm p}$ value of ^{65}As is negative and very small (-0.090 MeV) [18], corresponding to a loosely quasibound valence proton. The theoretical predictions suggest that the last valence proton in ^{65}As occupies the $2p_{3/2}$ orbit with low angular momentum $\ell = 1$ [19]. These imply that the very proton-rich nucleus ^{65}As probably has a proton-halo structure. In order to understand the exotic structure in this mass region, it is also of interest to investigate the neighboring nuclei ^{56,57}Cu, where the last valence proton is also located in the $2p_{3/2}$ orbit [10, 19].

The detailed results are listed in Table 2. In these three cases, the $R(2p_{3/2})$ values are generally larger than the $R_{\rm p}$ values by about 0.79 fm, and larger than the $R(1f_{5/2})$ [or $R(1f_{7/2})$] values by about 0.34 fm. These radial differences of 0.79 and 0.34 fm are smaller than those of ^{26,27,28}P, but more evident than that of ^{25}Al. This indicates that there could be proton skins or halos in ^{56,57}Cu and ^{65}As. Even though the $2p_{3/2}$ level is very loosely quasibound in ^{65}As, the $R(2p_{3/2})$ value is not significantly larger than the $R_{\rm p}$ value with respect to ^{56,57}Cu; this is attributed to the large Coulomb barrier in ^{65}As. In order to gain clear insight into their proton halos, we plot in Fig. 2 the radial density distributions of all protons, all neutrons, the last valence proton, and nuclear matter for the ground states of ^{56,57}Cu and ^{65}As. Similar to ^{26,27,28}P, the density distribution of the last valence proton makes a major contribution to the long tail forming in the proton density distribution. At the surface position, which is defined as the place where the density is half of the central density, the density of the last valence proton is found to be of the order of 10^{-3} g/cm^3. This is quite similar to the case of ^{26,27,28}P (one can see in Fig. 1 that the density of the last valence proton is also of the order of 10^{-3} g/cm^3 at the surface position). Thus it is concluded that there are proton halos in ^{56,57}Cu and ^{65}As. In fact, the present analysis is merely preliminary because the actual situation in ^{56,57}Cu and ^{65}As is more complex than what we consider here. In addition to the quasibound states with positive energies, deformation effects could affect the halo structure. Halos in deformed nuclei have attracted great interest in the last two decades. Hamamoto [29] performed mean-field calculations in axially symmetric quadrupole-deformed potentials. It was demonstrated in Ref. [29] that the $\ell = 0$ ($s_{1/2}$) component becomes dominant in the wave functions of neutron $\Omega^\pi = 1/2^+$ orbitals as the binding energy of the orbitals approaches zero, and hence no neutron $\Omega^\pi = 1/2^+$ orbitals contribute to deformation. Nunes [30] performed few-body calculations in the three-body model of a deformed core plus two neutrons and concluded that both nucleon-nucleon correlations and correlations due to deformation/excitation of the core inhibit the formation of halos. Zhou et al. [16] performed self-consistent mean-field calculations within the DRHB framework including the continuum, deformation effects, large spatial distributions, and the coupling among all these features. In contrast to Refs. [29, 30], deformed neutron halos were found in the deformed nucleus ^{44}Mg and the decoupling between the deformations of core and halo was discussed. Deformation effects are beyond the scope of this work.

Table 2. Structure properties calculated in the Woods-Saxon potential with fixed proton separation energies for the ground states of ^{56,57}Cu and ^{65}As. The energies are in MeV, and the radii are in fm. The values with error bars are the single-particle energies of the last valence proton $\varepsilon_{\ell j} = -S_{\rm p}(A,Z)$ and they are used to determine the potential depth V_0 in the Woods-Saxon potential.

	^{65}As	^{56}Cu	^{57}Cu
R_m	3.879	3.660	3.690
R_n	3.787	3.555	3.607
$R_{\rm p}$	3.967	3.755	3.770
$R(2p_{3/2})$	4.687	4.563	4.565
$R(1f_{5/2})$	4.354	4.216	–
$R(1f_{7/2})$	4.374	4.212	4.228
$\varepsilon(2p_{3/2})$(p)	0.090(85)[1]	-0.596(15)	-0.6903(4)
$\varepsilon(1f_{5/2})$(p)	0.063	-0.036	–
$\varepsilon(1f_{7/2})$(p)	-3.542	-4.234	-4.337
$\varepsilon(2s_{1/2})$(p)	-9.191	-10.537	-10.575
$\varepsilon(1d_{3/2})$(p)	-10.421	-11.504	-11.576
$\varepsilon(1d_{5/2})$(p)	-12.627	-14.117	-14.136
$\varepsilon(1p_{1/2})$(p)	-19.985	-22.095	-22.053
$\varepsilon(1p_{3/2})$(p)	-21.001	-23.316	-23.246
$\varepsilon(1s_{1/2})$(p)	-28.307	-31.448	-31.290
$\varepsilon(1f_{5/2})$(n)	-11.316	-11.459	-10.715
$\varepsilon(1f_{7/2})$(n)	-14.891	-15.758	-14.855
$\varepsilon(2s_{1/2})$(n)	-21.460	-22.954	-21.945
$\varepsilon(1d_{3/2})$(n)	-22.560	-23.850	-22.857
$\varepsilon(1d_{5/2})$(n)	-24.685	-26.444	-25.365
$\varepsilon(1p_{1/2})$(n)	-32.808	-35.229	-34.012
$\varepsilon(1p_{3/2})$(n)	-33.763	-36.414	-35.153
$\varepsilon(1s_{1/2})$(n)	-41.834	-45.353	-43.932

[1] Values as measured in the recent work Ref. [18].

So this leaves an open question concerning whether the possible proton halos in ^{56,57}Cu and ^{65}As are deformed or not. More complicated deformation calculations are worth performing in future modeling efforts.

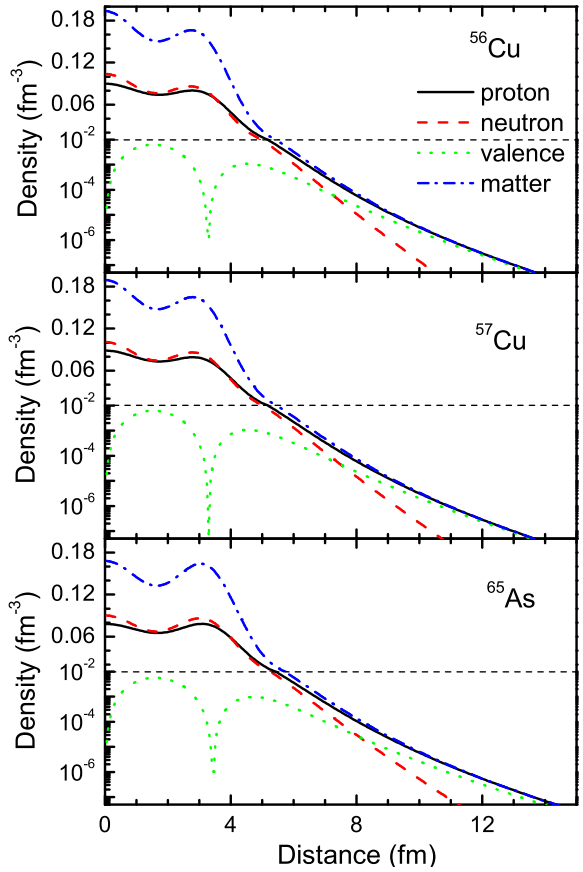

Fig. 2. (color online) Radial density probability distributions of all protons, all neutrons, the last valence proton, and nuclear matter, for the ground states of ^{56,57}Cu and ^{65}As. On the vertical axis, the density range of less than 0.01 g/cm^3 is shown in the logarithmic scale while the density range of more than 0.01 g/cm^3 is in the linear scale, and they are distinguished by thin dashed horizontal lines.

Ultimately, to clarify the properties of a halo proton, we plot in Fig. 3 the theoretical rms radius of the weakly bound or quasibound proton versus the proton separation energy for the $2s_{1/2}$ state in ^{26}P and the $2p_{3/2}$ state in ^{65}As. It is known that there is a significant inverse relation between the rms radius of a halo neutron in s-wave orbits and its neutron separation energy [26–28]. In contrast, this property is less evident for halo protons in s-wave orbits. As shown in Fig. 3, although the rms radius of the halo proton in ^{26}P is inversely related to the proton separation energy, the changes in the rms radius are small with respect to the halo neutron case. This is the case no matter whether the halo proton is bound or quasibound. The reason for this is that the additional repulsive Coulomb barrier plays an important role, which determines the behavior of the single-particle wave function in the asymptotic region. As the proton separation energy varies reasonably, corresponding to minor changes in the depth of the nuclear potential, the position and height of the Coulomb barrier remain almost the same. This leads to approximately the same behavior for the wave function in the external region. Hence, the rms radius of the halo proton, which is determined from the wave function, shows weak sensitivity to the proton separation energy. Besides the striking effect of the Coulomb barrier, it is also of interest to discern the effect of the centrifugal barrier. Let us compare the variation trends of the calculated rms radii for the $2s_{1/2}$ orbit in ^{26}P and the $2p_{3/2}$ orbit in ^{65}As. Obviously, when the last valence proton occupies the p-wave orbit rather than the s-wave orbit, the decrease of its rms radius is more gentle with increasing $S_{\rm p}$ values, as one would expect.

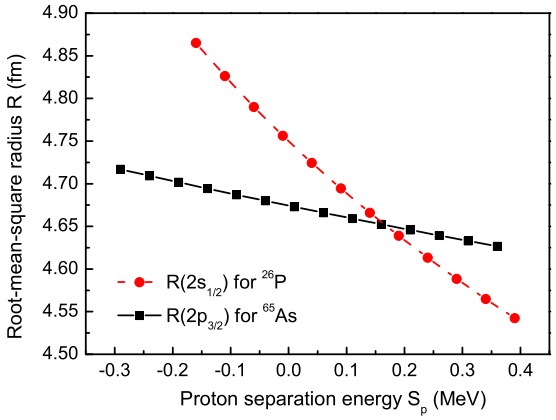

Fig. 3. (color online) Variations of the theoretical root-mean-square (rms) radius of the last valence proton for the $2s_{1/2}$ orbit in ^{26}P and the $2p_{3/2}$ orbit in ^{65}As.

4 Summary

In conclusion, we have presented a straightforward investigation of proton-halo structure in the very neutron-deficient F-P-Cu-As isotopes. The properties of various single-particle states, both bound and quasibound, are systematically calculated by the exact solution of the Schrödinger equation. The experimentally observed proton halos in the first excited state of ^{17}F and in the ground states of ^{26,27,28}P are reproduced well. Proton halos are predicted for the ground states of ^{56,57}Cu and ^{65}As as well. Moreover, in great contrast to neutron halos, proton halos show only weak sensitivity to the proton separation energy, no matter whether the last valence

proton is weakly bound or quasibound. The underlying reason is discussed, together with the influence of the ℓ=1 centrifugal barrier. It is of great interest and importance for experimentalists to search for proton halos or proton skins in more very proton-rich nuclei, which may guide theoretical studies. Efforts toward the complete understanding of proton halos are being made from both experimental and theoretical sides.

References

1 D. D. Ni and Z. Z. Ren, Phys. Lett. B, **744**: 22 (2015)
2 S. Åberg, P. B. Semmes, and W. Nazarewicz, Phys. Rev. C, **56**: 1762 (1997)
3 J. S. Al-Khalili and J. A. Tostevin, Phys. Rev. Lett., **76**: 3903 (1996)
4 J. L. Han et al, High Ener. Phys. Nucl. Phys., **30**: 1058 (2006)
5 Q. Wang et al, Chin. Phys. Lett., **23**: 1731 (2006)
6 D. D. Ni and Z. Z. Ren, Phys. Rev. C, **92**: 054322 (2015)
7 D. D. Ni and Z. Z. Ren, Phys. Rev. C, **93**: 054318 (2016)
8 Z. Z. Ren, B. Q. Chen, Z. Y. Ma, and G. O. Xu, Phys. Rev. C, **53**: R572 (1996)
9 Z. Z. Ren, A. Faessler, and A. Bobyk, Phys. Rev. C, **57**: 2752 (1998)
10 Z. Z. Ren, W. Mittig, and F. Sarazin, Nucl. Phys. A, **652**: 250 (1999)
11 S. S. Zhang, E. G. Zhao, and S. G. Zhou, Euro. Phys. J. A, **49**: 77 (2013)
12 B. A. Brown and P. G. Hansen, Phys. Lett. B, **381**: 391 (1996)
13 G. Hagen, T. Papenbrock, and M. Hjorth-Jensen, Phys. Rev. Lett., **104**: 182501 (2010)
14 J. Meng, H. Toki, S. G. Zhou, S. Q. Zhang, W. H. Long, and L. S. Geng, Prog. Part. Nucl. Phys., **57**: 470 (2006)
15 Y. Chen, P. Ring, and J. Meng, Phys. Rev. C, **89**: 014312 (2014)
16 S. G. Zhou, J. Meng, P. Ring, and E. G. Zhao, Phys. Rev. C, **82**: 011301(R) (2010)
17 L. L. Li, J. Meng, P. Ring, E. G. Zhao, and S. G. Zhou, Phys. Rev. C, **85**: 024312 (2012)
18 X. L. Tu et al, Phys. Rev. Lett., **106**: 112501 (2011)
19 G. Audi, F. G. Kondev, M. Wang, W. J. Huang, and S. Naimi, Chin. Phys. C, **41**: 030001 (2017)
20 S. Cwiok, J. Dudek, W. Nazarewicz, J. Skalski, and T. Werner, Comput. Phys. Commun., **46**: 379 (1987)
21 R. Morlock et al, Phys. Rev. Lett., **79**: 3837 (1997)
22 A. Navin et al, Phys. Rev. Lett., **81**: 5089 (1998)
23 Z. H. Liu, M. Ruan, Y. L. Zhao, H. Q. Zhang et al, Phys. Rev. C, **69**: 034326 (2004)
24 D. Q. Fang, W. Q. Shen, J. Feng et al, Eur. Phys. J. A, **12**: 335 (2001)
25 M. Wang, G. Audi, F. G. Kondev, W. J. Huang, S. Naimi, and X. Xu, Chin. Phys. C, **41**: 030003 (2017)
26 M. V. Zhukov, B. V. Danilin, D. V. Fedorov et al, Phys. Rep., **231**: 151 (1993)
27 T. Otsuka, N. Fukunishi, and H. Sagawa, Phys. Rev. Lett., **70**: 1385 (1993)
28 P. G. Hansen, Nucl. Phys. A, **553**: 89c (1993)
29 I. Hamamoto, Phys. Rev. C, **69**: 041306(R) (2004)
30 F. Nunes, Nucl. Phys. A, **757**: 349 (2005)